

Tunable Berry curvature dipole and hexapole in linearly polarized light-irradiated type-I semi-Dirac systems

Guo-Bao Zhu(朱国宝), Yun-Hai Zhang(张运海), Hui-Min Yang(杨慧敏)

Citation: Chin. Phys. B. 35, 097302 (2026). DOI: 10.1088/1674-1056/ae9528 |
CSTR: 32038.14.CPB.ae9528
http://cpb.iphy.ac.cn; http://iopscience.iop.org/cpb

What follows is a list of articles you may be interested in

Doping superlattices in conventional and wide-bandgap semiconductors: Physics, properties, and device applications

Xiao-Long Wu(武小龙), Geng-You Zhao(赵耕右), Bo Feng(冯博), Han-Ming Ding(丁汉明), Liang-Xue Gu(顾梁雪), Chuang Wang(王闯), Cheng Wang(王成), Kun Tang(汤琨), Shu-Ming Zhu(朱顺明), Jian-Dong Ye(叶建东), Shu-Lin Gu(顾书林)

Chin. Phys. B. 35, 097301 (2026). DOI: 10.1088/1674-1056/ae6d9a | CSTR: 32038.14.CPB.ae6d9a

Type-II Dirac nodal chain semimetal CrB_4

Xiao-Yao Hou(侯逍遥), Ze-Feng Gao(高泽峰), Peng-Jie Guo(郭朋杰), Jian-Feng Zhang(张建丰), Zhong-Yi Lu(卢仲毅)

Chin. Phys. B. 35, 017301 (2026). DOI: 10.1088/1674-1056/ae172b | CSTR: 32038.14.CPB.ae172b

Tunable colossal negative magnetoresistance of topological semimetal EuB_6 thin sheets

Ke Zhu(祝轲), Qi Qi(齐琦), Yaofeng Xie(谢耀锋), Lulu Pan(潘禄禄), Senhao Lv(吕森浩), Guojing Hu(胡国静), Zhen Zhao(赵振), Guoyu Xian(冼国裕), Yechao Han(韩烨超), Lihong Bao(鲍丽宏), Ying Zhang(张颖), Xiao Lin(林晓), Hui Guo(郭辉), Haitao Yang(杨海涛), Hong-Jun Gao(高鸿钧)

Chin. Phys. B. 34, 097308 (2025). DOI: 10.1088/1674-1056/add5ca | CSTR: 32038.14.CPB.add5ca

Emergence of metal–semiconductor phase transition in MX_2 (M = Ni, Pd, Pt; X = S, Se, Te) moiré superlattices

Jie Li(李杰), Rui-Zi Zhang(张瑞梓), Jinbo Pan(潘金波), Ping Chen(陈平), Shixuan Du(杜世萱)

Chin. Phys. B. 34, 037302 (2025). DOI: 10.1088/1674-1056/ada7d9 | CSTR: 32038.14.CPB.ada7d9

A universal resist-assisted metal transfer method for 2D semiconductor contacts

Xuanye Liu(刘轩冶), Linxuan Li(李林璇), Chijun Wei(尉驰俊), Peng Song(宋鹏), Hui Gao(高辉), Kang Wu(吴康), Nuertai Jiazila(努尔泰·加孜拉), Jiequn Sun(孙杰群), Hui Guo(郭辉), Haitao Yang(杨海涛), Wu Zhou(周武), Lihong Bao(鲍丽宏), Hong-Jun Gao(高鸿钧)

Chin. Phys. B. 33, 127302 (2024). DOI: 10.1088/1674-1056/ad8db4

Tunable Berry curvature dipole and hexapole in linearly polarized light-irradiated type-I semi-Dirac systems

Guo-Bao Zhu(朱国宝), Yun-Hai Zhang(张运海)†, and Hui-Min Yang(杨慧敏)

College of Physics and Electronic Engineering, Heze University, Heze 274015, *China*

(Received 10 May 2026; revised manuscript received 16 July 2026; accepted manuscript online 5 August 2026)

We investigate the effect of linearly polarized light (LPL) in type-I semi-Dirac (SD) systems. LPL can drive a transition between the single- and double-node phases in the system. Furthermore, the Berry curvature dipole (BCD) and Berry curvature hexapole (BCH) in the system change across the transition when the Fermi energy is near the band edge, while BCD and BCH can be suppressed by LPL when the Fermi energy moves away from the band edge. Moreover, the Berry curvature quadrupole (BCQ) is zero, regardless of whether LPL is present. These results will be useful for exploring the quantum geometry-driven nonlinear Hall effect in real materials.

Keywords: semi-Dirac system, Berry curvature dipole, Berry curvature hexapole, nonlinear transport

PACS: 73.43.–f, 73.43.Cd, 72.20.–i

DOI: 10.1088/1674-1056/ae9528 **CSTR:** 32038.14.CPB.ae9528

1. Introduction

Over the past several decades, Hall effects have emerged as an ideal probe for studying topological phases of matter. The Berry curvature (BC) is an essential ingredient in various topological phenomena. The BC is a geometrical property of an energy band that plays a key role in many physical phenomena. In time-reversal-breaking systems, both the quantum Hall effect and the quantum anomalous Hall effect are induced by BC.[1,2] Moreover, the BC plays a crucial role in tuning nonlinear transport properties in time-reversal-symmetric systems. For example, nonlinear Hall effects[3–5] can result from the product of a relaxation time scale and an average that incorporates the BC, the so-called Berry curvature dipole (BCD). BCD-driven nonlinear Hall effect requires broken space inversion symmetry and has attracted growing interest in recent years.[6–14] Recently, higher-order nonlinear anomalous Hall effects induced by Berry curvature multipoles such as quadrupole and hexapole have been discussed in certain materials with magnetic point group symmetry.[15,16] Probing and controlling the BC multipoles is becoming one of the main themes in the field of quantum materials.

Recently, two-dimensional semi-Dirac (SD) materials characterized by a quadratic dispersion in one direction and a linear dispersion along the orthogonal direction have been proposed.[17–31] Topological states with nonzero Chern number in an SD system can be induced by circularly polarized light.[21] In the presence of spin–orbit coupling, nontrivial topology with a nonzero Chern number emerges in an SD system.[26] An SD system with an inversion-symmetry-breaking mass exhibits nontrivial BC distribution, which generates an orbital magnetization and anomalous Nernst and thermal Hall conductivities.[30] The low-energy Dirac quasiparticles in an SD system can lead to a nonzero BCD.[31] However, the BC multipoles of SD systems in the presence of a mass term have rarely been taken into account.

On the other hand, another interesting class of topological states and topological phase transitions studied in recent years arises from manipulating nonequilibrium band structures under a periodic drive.[32–43] Several attempts have also been made to investigate the topological properties of type-I SD materials under the influence of either circularly or linearly polarized light (LPL).[21,27,28,30,43–46] Circularly polarized light can open a gap and induce topological states in a type-I SD system.[21] The type-I SD black phosphorus system can transit from a normal insulator to the Chern insulator phase when irradiated with circularly polarized light that satisfies the off-resonance condition.[44] Circularly polarized light opens a gap and induces a band inversion to create a finite Chern number in the SD system, while LPL can either open up a gap or split the semi-Dirac band-touching point into two Dirac points by an amount that depends on the amplitude of the light.[27] In previous studies, the effect of LPL on the intrinsic nonlinear Hall effect due to BC multipoles in an LPL-irradiated type-I SD system has rarely been explored.

Given this background, we have studied the effect of LPL in type-I SD systems. The system shows a transition between a single- and double-node phase due to LPL. The BCD and Berry curvature hexapole (BCH) in an SD system change across the transition when the Fermi energy is near the band edge, while BCD and BCH can be suppressed by LPL when the Fermi energy moves away from the band edge. Moreover, the Berry curvature quadrupole (BCQ) is zero, regardless of

†Corresponding author. E-mail: wlxzyh@163.com

© 2026 Chinese Physical Society and IOP Publishing Ltd. All rights, including for text and data mining, AI training, and similar technologies, are reserved.

whether LPL is present.

This paper is organized as follows. We first present the model Hamiltonian of a type-I SD system in the presence of LPL and analyze the band structures in Section 2. Based on these results, we further discuss the BCD, BCQ, and BCH of the LPL-irradiated type-I SD system in Section 3. Finally, we give a brief summary in Section 4.

2. Model and method

The low-energy electronic structure of a type-I SD system is given by the effective Hamiltonian[19–21,23]

$$H(\boldsymbol{k}) = (\alpha k_x^2 - \Delta)\sigma_x + v k_y \sigma_y + m_z \sigma_z, \tag{1}$$

where $\boldsymbol{k} = (k_x, k_y)$ is 2D momentum. α is the inverse of the quasiparticle mass along x, and v is the Dirac velocity along y. This means that SD fermions propagate as Galilean-invariant particles in one direction and as relativistic ones in the other direction, and the energy dispersion and Fermi surface of a type-I SD system are anisotropic. $\sigma_{x,y,z}$ are the Pauli matrices. Δ is a perturbation parameter and characterizes the difference between hopping energies in specific materials.[19,47] m_z describes the Dirac mass term, which breaks time-reversal symmetry.

When the system is subjected to LPL, the time-dependent Hamiltonian can be obtained by performing the Peierls substitution $\boldsymbol{k} \to \boldsymbol{k} + e\boldsymbol{A}(t)/\hbar$, where $\boldsymbol{A}(t)$ denotes the vector potential of the light. Specifically, the vector potential of LPL propagating along the z axis can be expressed as

$$\boldsymbol{A}(t) = A_0[\cos\omega t, \cos\omega t], \tag{2}$$

where ω is the frequency of the light and A_0 is the amplitude of the light. Generally speaking, the application of light to electron systems can dress the structures through mixing of different bands and redistribute electron occupation numbers through the absorption/emission of photons, which makes the system a nonequilibrium state. Based on Floquet theory,[39–43] an effective Hamiltonian under the application of light in the high-frequency limit can be obtained

$$H_{\text{eff}}(\boldsymbol{k}) = H_0(\boldsymbol{k}) + \frac{[H_{-1}, H_1]}{\hbar\omega} + \frac{[H_{-2}, H_2]}{2\hbar\omega}, \tag{3}$$

where

$$H_{\pm m} = \frac{\omega}{2\pi}\int_0^{\frac{2\pi}{\omega}} \mathrm{d}t H(t)\, \mathrm{e}^{\pm m\mathrm{i}\omega t}. \tag{4}$$

Straightforward calculations (see Appendix A for details) show that $[H_{-1}, H_1] = 0$ and $[H_{-2}, H_2] = 0$. The virtual photon processes[40] do not contribute to the effective Hamiltonian. As a result, the time-averaged Hamiltonian (H_0) dominates the time-dependent problem, and the corresponding static Floquet Hamiltonian of the type-I SD system is

$$H_{\text{eff}}(\boldsymbol{k}) = (\alpha k_x^2 - \Delta + \Delta_{\text{L}})\sigma_x + v k_y \sigma_y + m_z \sigma_z, \tag{5}$$

where $\Delta_{\text{L}} = \frac{\alpha e^2 A_0^2}{2\hbar^2}$. The corresponding energy dispersion is given by

$$E_{\pm} = \pm\sqrt{(\alpha k_x^2 - \Delta + \Delta_{\text{L}})^2 + v^2 k_y^2 + m_z^2}, \tag{6}$$

where $\pm$ denote the conduction and valence bands, respectively. In Fig. 1, we display the energy dispersions as a function of k_x for $k_y = 0$ at different parameters without (a/b/c) and with LPL (d). In the absence of the Dirac mass and LPL, the two energy bands touch at a single point at $\boldsymbol{k} = (0,0)$ when $\Delta = 0$, corresponding to a single-node semimetallic phase. When $\Delta > 0$, the node splits into two distinct band-touching points at $\boldsymbol{k} = (\pm\sqrt{\Delta/\alpha}, 0)$, leading to a double-node phase. As $\Delta < 0$, the nodes will be gapped out. Moreover, when a finite gap parameter m_z is introduced, no Dirac points survive, and the system no longer exhibits semimetallic behavior. Furthermore, when LPL is included, a single node appears at $\Delta = \Delta_{\text{L}}$ for $\Delta > 0$. LPL can drive the transition between single-node and double-node phases. Each phase shows a different band structure, and the distribution of BC will change. As a consequence, the quantum geometric quantities and nonlinear transport properties can be modified by LPL.

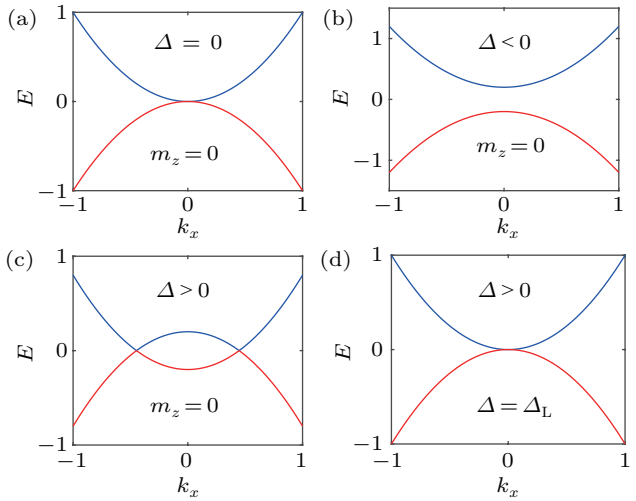


Fig. 1. Energy dispersions as a function of k_x for $k_y = 0$ at different parameters without (a/b/c) and with linearly polarized light (d). The parameters are set as follows: (a) $\Delta = 0$, $m_z = 0$; (b) $\Delta < 0$, $m_z = 0$; (c) $\Delta > 0$, $m_z = 0$; and (d) $\Delta > 0$, $\Delta = \Delta_{\text{L}}$, $m_z = 0$.

3. Berry curvature multipoles induced nonlinear anomalous Hall effect

Based on the semiclassical Boltzmann equation,[1,2] the anomalous Hall conductance resulting from the anomalous velocity due to BC is

$$\sigma_{ab} = -e^2 \varepsilon_{abz} \sum_n \int \mathrm{d}^2\boldsymbol{k} f_0(E_n(k)) \Omega_z^n(k), \tag{7}$$

where ε_{abc} $(a,b,c = x,y,z)$ is the Levi–Civita symbol. Ω_z^n is the BC corresponding to band $E_n(k)$, and $f_0(E_n(k))$ is the

Fermi–Dirac distribution. By recursively solving the semi-classical Boltzmann equation, the high-order anomalous Hall conductance contributed by higher moments of BC is[5,15,16]

$$\sigma^{(n\omega)}_{\mu\alpha_1\alpha_2\cdots\alpha_n} = \frac{2e(-\frac{e}{2\hbar})^2}{\prod_{m=1}^{n-1}\widetilde{m\omega}}\varepsilon_{\mu\alpha_1\beta}P_{\alpha_2\alpha_3\cdots\alpha_n\beta}, \tag{8}$$

where $\widetilde{m\omega} = \mathrm{i}m\omega + 1/\tau$, ω is the frequency of the driving electric field, τ is the phenomenological transport relaxation time of electrons, and the $(n-1)$th Berry curvature moment is

$$P_{\alpha_2\alpha_3\cdots\alpha_n\beta} = \int \frac{\mathrm{d}^2\boldsymbol{k}}{(2\pi)^2} f_0 \partial_{\alpha_2}\partial_{\alpha_3}\cdots\partial_{\alpha_n}\Omega_\beta(k). \tag{9}$$

3.1. Berry curvature dipoles

The BCD can also be rewritten as

$$D_{bd} = \int \frac{\mathrm{d}^2\boldsymbol{k}}{(2\pi)^2}\sum_n v_b^n \Omega_d^n(k)\left(-\frac{\partial f_0(k)}{\partial E}\right)_{E=E_n(k)}, \tag{10}$$

where v_b^n is the group velocity component for band $E_n(k)$. In a two-level system, the Hamiltonian can be written in the basis of the identity matrix and the three Pauli matrices,

$$H(\boldsymbol{k}) = \boldsymbol{d}(\boldsymbol{k})\cdot\hat{\boldsymbol{\sigma}} + d_0(\boldsymbol{k})\sigma_0, \tag{11}$$

where $\boldsymbol{d}(\boldsymbol{k}) = (d_x(\boldsymbol{k}), d_y(\boldsymbol{k}), d_z(\boldsymbol{k}))$ and $\hat{\boldsymbol{\sigma}} = (\sigma_x, \sigma_y, \sigma_z)$. The corresponding BC of the valence band along the z direction can be written as[48,49]

$$\Omega_z(\boldsymbol{k}) = -\frac{1}{2}\frac{\boldsymbol{d}}{d^3}\cdot\left(\frac{\partial \boldsymbol{d}}{\partial k_x}\times\frac{\partial \boldsymbol{d}}{\partial k_y}\right), \tag{12}$$

where $d = |\boldsymbol{d}|$. For the light-irradiated type-I SD system, $d_x = \alpha k_x^2 - \Delta + \Delta_{\mathrm{L}}$, $d_y = vk_y$, and $d_z = m_z$. Straightforward calculations show that the BC is

$$\Omega_z^{\pm}(\boldsymbol{k}) = \pm\frac{v}{2}\frac{2\alpha m_z k_x}{[(\alpha k_x^2 - \Delta + \Delta_{\mathrm{L}})^2 + v^2k_y^2 + m_z^2]^{\frac{3}{2}}}. \tag{13}$$

$\Omega_z^{\pm}$ is an odd function of k_x. Consequently, the total BC integrated over the Brillouin zone vanishes, and the Chern number is zero, regardless of whether LPL is present.

In the light-irradiated type-I SD system, the velocity components are

$$v_x^{\pm} = \frac{2\alpha k_x(\alpha k_x^2 - \Delta + \Delta_{\mathrm{L}})}{E_{\pm}}, \tag{14}$$

$$v_y^{\pm} = \frac{v^2 k_y}{E_{\pm}}. \tag{15}$$

$v_y^{\pm}$ is an odd function of k_y. Thus, the integrand $v_y^{\pm}\Omega_z^{\pm}$ for the y component of BCD Eq. (10) becomes an odd function under momentum inversion and suppresses D_{yz}. This is consistent with the underlying mirror symmetry M_x, which forbids any BCD response along the y direction,[5] and BCD does not lead to a transverse current when the electric field is along the y direction, regardless of whether LPL is present.

For the x component, the integrand $v_x^{\pm}\Omega_z^{\pm}$ contributes a finite value of D_{xz}. Therefore, when the electric field is applied along the x direction, BCD induces a charge current flowing along the y direction. When LPL is absent, Samal *et al.*[31] have shown that D_{xz} is independent of the Dirac velocity and predominantly depends on the inverse of the effective mass of the Dirac quasiparticles, as compared to typical isotropic Dirac systems with well-separated Dirac nodes. In Fig. 2(a), we show the Berry curvature dipole D_{xz} as a function of the Fermi energy E_{F} under LPL for different values of Δ_{L} at fixed $\Delta = 0.2\alpha$ and $m_z = 0.1\alpha$ at zero temperature. When E_{F} lies inside the bulk gap, D_{xz} vanishes as the BCD is a Fermi surface property. The response reaches its maximum value near the band edge as the BC becomes maximum at the band edges (see Eq. (13)), and it vanishes as $E_{\mathrm{F}} \to \infty$. Furthermore, the magnitude and profile of the response further depend on $\Delta_{\mathrm{L}}\alpha$. Near the band edge, $v_x^{\pm}\Omega_z^{\pm} = 2v\alpha m_z k_x^2 d_x/E_{\pm}^4$ is concentrated around $k_x^{\pm} = \pm\sqrt{(\Delta - \Delta_{\mathrm{L}})/\alpha}$, where $v_x^{\pm}\Omega_z^{\pm}$ shown in Fig. 2(b) forms a dipole-like structure with opposite signs. As a result, the net dipole contribution is significantly reduced compared with the case $\Delta_{\mathrm{L}} = 0.2\alpha$. When the Fermi energy moves away from the band edge, the amplitude of D_{xz} can be suppressed by increasing Δ_{L}.

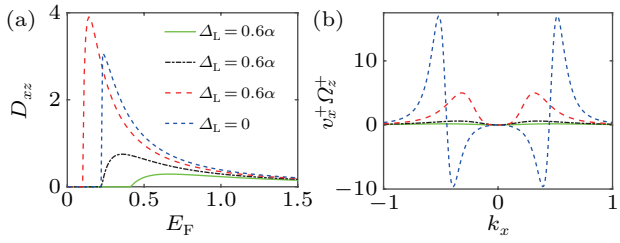


Fig. 2. (a) Plot of the Berry curvature dipole D_{xz} as a function of the Fermi energy E_{F} under LPL for different values of Δ_{L} at fixed $\Delta = 0.2\alpha$ and $m_z = 0.1\alpha$. (b) Density plots showing the Berry curvature Ω_z^+ multiplied by the velocity component v_x^+ in the $k_y = 0$ plane for different values of Δ_{L} with fixed $\Delta = 0.2\alpha$ and $m_z = 0.1\alpha$. The blue dotted, red dashed, black dash-dotted, and green solid curves correspond to $\Delta_{\mathrm{L}} = 0$, $\Delta_{\mathrm{L}} = 0.2\alpha$, $\Delta_{\mathrm{L}} = 0.4\alpha$, and $\Delta_{\mathrm{L}} = 0.6\alpha$, respectively. α is set to 1.

3.2. Berry curvature quadrupole

When the BC is forced to align along the z direction, the BCQ can be denoted as

$$Q_{ab} = \int \frac{d^2\boldsymbol{k}}{(2\pi)^2}\sum_n v_a^n \frac{\partial\Omega_z^n(k)}{\partial k_{\mathrm{b}}}\left(-\frac{\partial f_0(k)}{\partial E}\right)_{E=E_n(k)}. \tag{16}$$

In the present model, we obtain

$$\frac{\partial\Omega_z^{\pm}}{\partial k_x} = \frac{v\alpha m_z}{E_{\pm}^3}\left[1 - \frac{6\alpha k_x^2(\alpha k_x^2 - \Delta + \Delta_{\mathrm{L}})}{E_{\pm}^2}\right], \tag{17}$$

$$\frac{\partial\Omega_z^{\pm}}{\partial k_y} = -\frac{3v^3k_y}{2}\frac{2\alpha m_z k_x}{E_{\pm}^5}. \tag{18}$$

$v_x^{\pm}\frac{\partial\Omega_z^{\pm}(k)}{\partial k_x}$, $v_x^{\pm}\frac{\partial\Omega_z^{\pm}(k)}{\partial k_y}$, and $v_y^{\pm}\frac{\partial\Omega_z^{\pm}(k)}{\partial k_y}$ are odd functions of k_x, k_y, and k_x, respectively. Their integrals over k at zero temperature are zero. Therefore, the BCQ does not induce a charge current in an SD system, regardless of whether LPL is present.

3.3. Berry curvature hexapole

When the BC is forced to align along the z direction, the BCH can be denoted as

$$H_{abc} = \int \frac{d^2\boldsymbol{k}}{(2\pi)^2} \sum_n v_a^n \frac{\partial^2 \Omega_z^n(k)}{\partial k_b \partial k_c} \left(-\frac{\partial f_0(k)}{\partial E}\right)_{E=E_n(k)}. \quad (19)$$

There are four independent components of BCH: H_{xxx}, H_{xxy}, H_{xyy}, and H_{yyy}. In the present model, we obtain

$$\frac{\partial^2 \Omega_z^{\pm}}{\partial k_x^2} = -\frac{6v m_z \alpha^2 k_x (5\alpha k_x^2 - 3\Delta + 3\Delta_{\rm L})}{E_{\pm}^5} + \frac{60 v m_z \alpha^3 k_x^3 (\alpha k_x^2 - \Delta + \Delta_{\rm L})^2}{E_{\pm}^7}, \quad (20)$$

$$\frac{\partial^2 \Omega_z^{\pm}}{\partial k_x \partial k_y} = -\frac{3v^3 \alpha m_z k_y}{E_{\pm}^5}\left[1 - \frac{10\alpha k_x^2(\alpha k_x^2 - \Delta + \Delta_{\rm L})}{E_{\pm}^2}\right], \quad (21)$$

$$\frac{\partial^2 \Omega_z^{\pm}}{\partial k_y^2} = -\frac{3v^3 \alpha m_z k_x}{E_{\pm}^5}\left(1 - \frac{5v^2 k_y^2}{E_{\pm}^2}\right). \quad (22)$$

$v_x^{\pm}\frac{\partial^2 \Omega_z^{\pm}}{\partial k_x \partial k_y}$ and $v_y^{\pm}\frac{\partial^2 \Omega_z^{\pm}}{\partial k_y^2}$ are odd functions of k_x and k_y, respectively. Their integrals over k at zero temperature are zero. Therefore, H_{xxy} and H_{yyy} are zero, while H_{xxx} and H_{xyy} are nonzero, regardless of whether LPL is present. Furthermore, when the electric field is applied along the x direction, BCH generates a fourth-harmonic voltage flowing along the y direction, while BCH does not lead to a fourth-harmonic voltage when the electric field is along the y direction. When the electric field is not applied along either of the two axes, BCH will have additional contributions to the anomalous Hall voltage.

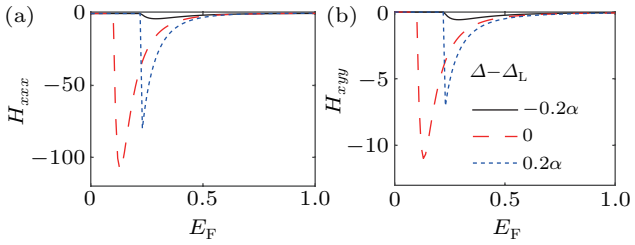


Fig. 3. (a) and (b) Plots of the Berry curvature hexapole H_{xxx}/H_{xyy} as a function of the Fermi energy $E_{\rm F}$ for different values of $\Delta - \Delta_{\rm L}$ at fixed $m_z = 0.1\alpha$. The black solid, red dashed, and blue dotted curves correspond to $\Delta - \Delta_{\rm L} = -0.2\alpha$, $\Delta - \Delta_{\rm L} = 0$, and $\Delta - \Delta_{\rm L} = 0.2\alpha$, respectively. α is set to 1.

Figures 3(a) and 3(b) show H_{xxx} and H_{xyy} as a function of the Fermi energy $E_{\rm F}$ for different values of $\Delta - \Delta_{\rm L}$ at fixed $m_z = 0.1\alpha$, respectively. When $E_{\rm F}$ lies inside the bulk gap, H_{xxx} and H_{xyy} vanish. This behavior of H_{xxx} and H_{xyy} is a Fermi surface property, which is the same as that of the BCD. H_{xxx} and H_{xyy} show a peak at the band edges and vanish when $E_{\rm F} \to \infty$, which results from the dependence of $v_x^n \frac{\partial^2 \Omega_z^n(k)}{\partial k_i \partial k_i}$ on higher orders of $1/E_{\rm F}$. Based on Eqs. (20) and (21), the magnitude and profile of H_{xxx} and H_{xyy} can be controlled by the interplay between Δ and m_z. For fixed Δ, the magnitude and profile of H_{xxx} and H_{xyy} can be suppressed by increasing $\Delta_{\rm L}$ when the Fermi energy moves away from the band edge, in contrast to the case when the Fermi energy is near the band edge.

4. Summary

In summary, we have studied the Berry curvature multipoles and band structure in a type-I semi-Dirac system under LPL. By tuning the LPL, the system shows a transition between a single- and double-node phase. The x component of the BCD is finite, while the y component is zero. This means that when the electric field is applied along the x direction, BCD induces a charge current flowing along the y direction, while BCD does not lead to a transverse current when the electric field is along the y direction. The two components H_{xxx} and H_{xyy} of the BCH are finite. These results show that the BCH generates a fourth-harmonic voltage flowing along the y direction when the electric field is applied along the x direction, and has additional contributions to the anomalous Hall voltage when the electric field is not applied along either of the two axes. Furthermore, the BCD and BCH in the system change across the transition induced by LPL when the Fermi energy is near the band edge, while BCD and BCH can be suppressed by LPL when the Fermi energy moves away from the band edge. Moreover, the BCQ is zero, regardless of whether LPL is present. These results will be useful for controlling quantum geometry-driven nonlinear transport phenomena.

Appendix A: Floquet Hamiltonian

In Eq. (4), when linearly polarized light is included, we obtain

$$H_{\pm m} = \frac{1}{T}\int_0^T {\rm d}t\, {\rm e}^{\pm {\rm i}m\omega t}(H(\boldsymbol{k}) + H_t^x\sigma_x + H_t^y\sigma_y), \quad (A1)$$

$$H_t^x = 2\alpha\kappa k_x \cos\omega t + \alpha\kappa^2\cos^2\omega t, \quad (A2)$$

$$H_t^y = v\kappa\cos\omega t, \quad (A3)$$

with $\kappa = eA_0/\hbar$. We obtain

$$H_0 = H(\boldsymbol{k}) + \frac{\alpha\kappa^2}{2}\sigma_x, \quad (A4)$$

$$H_{\pm 1} = \alpha\kappa k_x\sigma_x + \frac{1}{2}\eta v\kappa\sigma_y, \quad (A5)$$

$$H_{\pm 2} = \frac{1}{4}\sigma_x, \quad (A6)$$

where we have used the relations

$$\frac{1}{T}\int_0^T {\rm d}t\cos\omega t = 0,\ \frac{1}{T}\int_0^T {\rm d}t\cos^2\omega t = \frac{1}{2},$$
$$\frac{1}{T}\int_0^T {\rm d}t\, {\rm e}^{\pm {\rm i}\omega t}\cos\omega t = \frac{1}{2},\ \frac{1}{T}\int_0^T {\rm d}t\, {\rm e}^{\pm {\rm i}\omega t}\cos^2\omega t = 0,$$
$$\frac{1}{T}\int_0^T {\rm d}t\, {\rm e}^{\pm 2{\rm i}\omega t}\cos\omega t = 0,\ \frac{1}{T}\int_0^T {\rm d}t\, {\rm e}^{\pm 2{\rm i}\omega t}\cos^2\omega t = \frac{1}{4}.$$

Then, we obtain

$$[H_{-1}, H_1] = 0, \tag{A7}$$

$$[H_{-2}, H_2] = 0. \tag{A8}$$

Finally, the Floquet Hamiltonian of the type-I SD system is

$$H_{\text{eff}}(\boldsymbol{k}) = \left(\alpha k_x^2 - \Delta + \frac{\alpha\kappa^2}{2}\right)\sigma_x + v k_y \sigma_y + m_z \sigma_z. \tag{A9}$$

Acknowledgment

Project supported by Shandong Provincial Natural Science Foundation (Grant No. ZR2021MA093).

References

[1] Xiao D, Chang M C and Niu Q 2010 *Rev. Mod. Phys.* **82** 1959
[2] Nagaosa N, Sinova J, Onoda S, MacDonald A H and Ong N P 2010 *Rev. Mod. Phys.* **82** 1539
[3] Rostami H and Juričić V 2020 *Phys. Rev. Res.* **2** 013069
[4] Du Z Z, Lu H Z and Xie X C 2021 *Nat. Rev. Phys.* **3** 744
[5] Sodemann I and Fu L 2015 *Phys. Rev. Lett.* **115** 216806
[6] Lee J, Wang Z, Xie H, Mak K F and Shan J 2017 *Nat. Mater.* **16** 887
[7] Son J, Kim K H, Ahn Y H, Lee H W and Lee J 2019 *Phys. Rev. Lett.* **123** 036806
[8] He P, Isobe H, Zhu D, Hsu C H, Fu L and Yang H 2021 *Nat. Commun.* **12** 698
[9] Ho S C, Chang C H, Hsieh Y C, Lo S T, Huang B, Vu T H Y, Ortix C and Chen T M 2021 *Nat. Electron.* **4** 116
[10] Duan J, Jian Y, Gao Y, Peng H, Zhong J, Feng Q, Mao J and Yao Y 2022 *Phys. Rev. Lett.* **129** 186801
[11] Zhang C P, Xiao J, Zhou B T, Hu J X, Xie Y M, Yan B and Law K T 2022 *Phys. Rev. B* **106** L041111
[12] Sinha S, Adak P C, Chakraborty A, Das K, Debnath K, Sangani L V, Watanabe K, Taniguchi T, Waghmare U V, Agarwal A and Deshmukh M M 2022 *Nat. Phys.* **18** 765
[13] Huang M, Wu Z, Zhang X, Feng X, Zhou Z, Wang S, Chen Y, Cheng C, Sun K, Meng Z Y and Wang N 2023 *Phys. Rev. Lett.* **131** 066301
[14] Zhao T Y, Wang A Q, Ye X G, Liu X Y, Liao X and Liao Z M 2023 *Phys. Rev. Lett.* **131** 186302
[15] Parker D E, Morimoto T, Orenstein J and Moore J E 2019 *Phys. Rev. B* **99** 045121
[16] Zhang C P, Gao X J, Xie Y M, Po H C and Law K T 2023 *Phys. Rev. B* **107** 115142
[17] Dietl P, Piéchon F and Montambaux G 2008 *Phys. Rev. Lett.* **100** 236405
[18] Banerjee S, Singh R R P, Pardo V and Pickett W E 2009 *Phys. Rev. Lett.* **103** 016402
[19] Montambaux G, Piéchon F, Fuchs J N and Goerbig M O 2009 *Phys. Rev. B* **80** 153412
[20] Delplace P and Montambaux G 2010 *Phys. Rev. B* **82** 035438
[21] Saha K 2016 *Phys. Rev. B* **94** 081103
[22] Kotov V N, Uchoa B and Sushkov O P 2021 *Phys. Rev. B* **103** 045403
[23] Rostamzadeh S and Sarisaman M 2022 *New J. Phys.* **24** 083026
[24] Asafov D and Pavlov I 2024 *Phys. Rev. B* **110** 125126
[25] Carbotte J P and Nicol E J 2019 *Phys. Rev. B* **100** 035441
[26] Huang H, Liu Z, Zhang H, Duan W and Vanderbilt D 2015 *Phys. Rev. B* **92** 161115
[27] Chen Q, Du L and Fiete G A 2018 *Phys. Rev. B* **97** 035422
[28] Islam S K F and Saha A 2018 *Phys. Rev. B* **98** 235424
[29] Carbotte J P, Bryenton K R and Nicol E J 2019 *Phys. Rev. B* **99** 115406
[30] Vargiamidis V, Vasilopoulos P and Neophytou N 2025 *Phys. Rev. B* **112** 045406
[31] Samal S S, Nandy S and Saha K 2021 *Phys. Rev. B* **103** L201202
[32] Eckardt A 2017 *Rev. Mod. Phys.* **89** 011004
[33] Weitenberg C and Simonet J 2021 *Nat. Phys.* **17** 1342
[34] Vogl M, Laurell P, Barr A D and Fiete G A 2019 *Phys. Rev. X* **9** 021037
[35] Rudner M S and Lindner N H 2020 *Nat. Rev. Phys.* **2** 229
[36] Harper F, Roy R, Rudner M S and Sondhi S L 2020 *Annu. Rev. Condens. Matter Phys.* **11** 345
[37] Bao C, Tang P, Sun D and Zhou S 2022 *Nat. Rev. Phys.* **4** 33
[38] Mori T 2023 *Annu. Rev. Condens. Matter Phys.* **14** 35
[39] Oka T and Aoki H 2009 *Phys. Rev. B* **79** 081406
[40] Kitagawa T, Oka T, Brataas A, Fu L and Demler E 2011 *Phys. Rev. B* **84** 235108
[41] Ezawa M 2013 *Phys. Rev. Lett.* **110** 026603
[42] Bhattacharya A and Islam S F 2021 *Phys. Rev. B* **104** L081411
[43] Chen J N, Yang Y Y, Zhou Y L, Wu Y J, Duan H J, Deng M X and Wang R Q 2022 *Phys. Rev. B* **105** 085124
[44] Sengupta P and Jauregui L A 2021 *J. Appl. Phys.* **130** 054303
[45] Ghosh B, Bandyopadhyay M and Nandy S 2026 arXiv:2603.00146 [cond-mat.mes-hall]
[46] Zeng W 2026 arXiv:2603.00944 [cond-mat.supr-con]
[47] Montambaux G, Piéchon F, Fuchs J N and Goerbig M O 2009 *Eur. Phys. J. B* **72** 509
[48] Qi X L, Hughes T L and Zhang S C 2008 *Phys. Rev. B* **78** 195424
[49] Sticlet D, Piéchon F, Fuchs J N, Kalugin P and Simon P 2012 *Phys. Rev. B* **85** 165456